World Applied Sciences Journal 25 (2): 288-293, 2013
ISSN 1818-4952

DOI: 10.5829/idosi.wasj.2013.25.02.2931

Mathematical Modeling of Biohydrogen Production in an EGSB Reactor Utilizing Computational Fluid Dynamics

Leila Vafajoo and Behrooz beigy

Chemical and Environmental Group, Fanni College,
Islamic Azad University, South Tehran Branch, Tehran, Iran

Submitted: Jul 25, 2013; **Accepted:** Sep 4, 2013; **Published:** Oct 1, 2013

Abstract: In this study the performance of an Expanded Granular Sludge Bed (EGSB) reactor for biological production of ethanol and hydrogen was modeled using computational fluid dynamics. The effect of different Hydraulic Retention Time (HRT) of 1, 2 and 4 hr and Glucose mass fraction in feed of 0.002, 0.004, 0.006 and 0.008 on Hydrogen and ethanol production rate was determined. The maximum value of H2 production rate at the HRT of equal to 2h and Glucose mass fraction of 0.008 is 0.033 kg/h. It was demonstrated that the model is capable of predicting the variation of the EGSB reactor performance for biohydrogen and bioethanol production at various substrate concentrations and HRT values.

Key words: EGSB reactor · Biohydrogen Production · Modeling, Bioethanol · Computational Fluid Dynamics

INTRODUCTION

One of the most important challenges of the current century is to develop new sources of renewable energies which might be able to replace fossil fuels. An ideal replacement would be a clean fuel that has a high efficiency of conversion. Hydrogen is a promising fuel because it is clean, renewable and has a high energy density of 122 kJ/g [1]. Currently, hydrogen is produced by electrolysis of water or by steam reformation of methane amongst other techniques. Unfortunately, most of these processes are highly energy intensive, making hydrogen production very expensive [2, 3].

Biological H_2 production as an alternative route is more attractive especially when organic wastewater or other wastes are used as raw materials. Biological processes are particularly useful because they are catalyzed by microorganisms at environmental temperature and pressure and they require low energy investments, which makes them attractive as alternatives to conventional physical/chemical methods of H^2 production. In addition, these techniques are well suited for decentralized energy production at plants where small-scale biomass or waste are available, thus avoiding the expenses and energy costs of transport [4].

Under anaerobic conditions, hydrogen is produced as a by-product during the conversion of organic wastes into organic acids, which are then used for methane generation. The acidogenic phase of anaerobic digestion can be manipulated to improve H_2 production [2,3]. The anaerobic digestion is a multi-step process consisting of hydrolysis of complex organic substrates such as proteins, lipids and carbohydrates into soluble amino acids, fatty acids and sugars followed by the fermentation to acetate, format, hydrogen and carbon dioxide, which are finally utilized by methanogenic microorganisms to form methane.

Anaerobic reactors such as upflow anaerobic sludge blanket (UASB), expanded granular sludge bed (EGSB) and anaerobic fluidized bed (AFB) reactors are commonly used for the biological processes. There are clear differences between UASB, EGSB and AFB reactors as shows in Table 1 [1,4,5,6,7].

The EGSB reactor, a three-phase system, has been widely used for the treatment of wastewater due to its high operational efficiency even at high organic loading rates (OLR) and heavy biomass accumulation on the support media [4]. Although an EGSB bioreactor has been used in biochemical applications for many years, but a restricted research have been published on its

Corresponding Author: Leila Vafajoo and Behrooz beigy, Chemical and Environmental Group, Fanni College, Islamic Azad University, South Tehran Branch, Tehran, Iran.

Table 1: Comparison of UASB, EGSB, and AFB reactors [1,4,5,6,7]

Reactortype	Fluid Superficialvelocity	Dead volume	Recirculation Flow	Height/diameterratio	Grannuls diameter	Flowpattern
UASB	Low	high	None	Low	High	Plug flow
EGSB	High	low	High	Medium	Low	Completemixed
AFBR	High	low	medium	High	High	Completemixed

mathematical modeling. Because of the higher upflow velocities, which are caused by a high recycle rate and the sludge expansion through the whole reactor, which is caused by high height/diameter ratio, an EGSB reactor has minimum reactor dead volume.

Mathematical Modelin: Biochemical reaction: In this work, it is assumed that the fermentation process will immediately take place as the water is contacted with the sludge phase in a reactor with height of 120 cm and the internal diameter of 6 cm [8]. The species reaction model was implemented to determine the mass fractions of glucose, ethanol, acetic acid, carbon dioxide and hydrogen resulting from glucose fermentation, *i.e.*

$$C_6H_{12}O_6 + H_2O \rightarrow CH_3COOH + CH_3CH_2OH + 2H_2 + 2CO_2 \quad (1)$$

The rate equation for the reaction is written as:

$$R = -kC_{C_6H_{12}O_6} \quad (2)$$

With the reaction rate constant of 2.06 h^{-1} [7].

Methodology for Computational Fluid Dynamics Model Generation: In this research, a two-dimensional Eulerian-Eulerian three-phase fluid model has been employed to describe the flow behavior of each phase, so the biogas, wastewater and sludge granules are all treated as different continua and they were assumed to be incompressible.

The wastewater was regarded as mixed liquid, initially containing pure water with different mass fraction of glucose from 0.002 to 0.008 and the density was determined by volume weighted mixing law. The sludge granules took up about 40% of the volume in the bed region and are considered to be spherical solid granules with a density of 1460 $kg.m^{-3}$, diameter of 1 mm and dynamic viscosity of 0.005 $kg.m^{-1}s^{-1}$. The gas phase volume fraction was related to gas production in reaction and the gas bubbles were assumed to have a diameter of 0.1 mm. The biogas was assumed to have a density of 1.139 $kg.m^{-3}$ and a dynamic viscosity of 0.019 $kg.m^{-1}s^{-1}$ [8,9].

Turbulence Modeling of the Continuous Phase: The turbulence modeling of the continuous phase is based on the two-equation (k,ε) turbulence model derived in a three-phase flow, including the interfacial transfer of turbulent kinetic energy and its dissipation rate. The Reynolds stress tensor for the continuous phase q has the following form:

$$\bar{\bar{\tau}}_q = -\frac{2}{3}(\rho_q k_q + \rho_q \mu_{t,q} \nabla . \vec{U}_q)\bar{\bar{I}} + \rho_q \mu_{t,q}(\nabla \vec{U}_q + \nabla \vec{U}_q^T) \quad (3)$$

Where U_q is the phase-weighted velocity. The turbulent viscosity $\mu_{t,q}$ is written in terms of the turbulent kinetic energy of phase q:

$$\mu_{t,q} = \rho_q C_\mu \frac{K_q^2}{\varepsilon_q} \quad (4)$$

the kq transport equation in phase q is expressed as:

$$\frac{\partial}{\partial t}(\alpha_q \rho_q k_q) + \nabla .(\alpha_q \rho_q \vec{U}_q k_q) = \nabla .(\alpha_q \frac{\mu_{t,q}}{\sigma_k} \nabla k_q) + \alpha_q G_{k,q} - \alpha_q \rho_q \varepsilon_q + \alpha_q \rho_q \prod_{k_q} \quad (5)$$

The transport equation of the dissipation rate of ε_q in the phase q is expressed as:

$$\frac{\partial}{\partial t}(\alpha_q \rho_q \varepsilon_q) + \nabla .(\alpha_q \rho_q \vec{U}_q \varepsilon_q) = \nabla .(\alpha_q \frac{\mu_{t,q}}{\sigma_\varepsilon} \nabla \varepsilon_q) + \alpha_q \frac{\varepsilon_q}{k_q}(C_{1\varepsilon} G_{k,q} - C_{2\varepsilon} \rho_q \varepsilon_q) + \alpha_q \rho_q \prod_{\varepsilon_q} \quad (6)$$

Here Π_{Kq} and $\Pi_{\varepsilon q}$ represent the influence of the dispersed phases on the continuous phase q and $G_{K,q}$ is the production of turbulent kinetic energy ; σ_k and $\sigma\varepsilon$ are the turbulent Prantdle numbers for K and ε, respectively. The term Π_{Kq} can be derived from the instantaneous equation of the continuous phase and takes the following form, where M represents the number of secondary phases:

$$\Pi_{k_q} = \sum_{p=1}^{M} \frac{K_{pq}}{\alpha_q \rho_q}(k_{pq} - 2k_q + \vec{v}_{pq}.\vec{v}_{dr}) \quad (7)$$

where k_{lq} is the covariance of the velocities of the locity and v_{dr} is the drift velocity. $\Pi_{\varepsilon q}$ is modeled according to: continuous phase q and the dispersed phase l), v_{pq} is the relative veocity.

$$\Pi_{\varepsilon_q} = C_{3\varepsilon}\frac{\varepsilon_q}{k_q}\Pi_{k_q} \quad (8)$$

In this study, $C_{1\varepsilon}$, $C_{2\varepsilon}$ and $C_{3\varepsilon}$ are constant and equal to 1.44, 1.92 and 1.2, respectively [9].

Interphase Momentum Transfer: In this study, only drag forces and lift forces between the continuous phase and the dispersed phase are considered. The drag forces exerted by the dispersed phase on the continuous phase are calculated as:

$$M_{D,ls} = \frac{3}{4}\frac{C_{D,ls}}{d_s}\rho_l \alpha_s \left|u_S - u_l\right|(u_S - u_l) \quad (9)$$

$$M_{D,\lg} = \frac{3}{4}\frac{C_{D,\lg}}{d_g}\rho_l \alpha_g \left|u_g - u_l\right|(u_g - u_l) \quad (10)$$

Where CD is the drag coefficient and d is the diameter. The drag coefficient exerted by the gas phase on the liquid phase, $C_{D,lg}$ is obtained as follows:

$$C_{D,\lg} = \begin{cases} \dfrac{24(1+0.15(1-\alpha_g)\mathrm{Re}^{0.687})}{(1-\alpha_g)\mathrm{Re}} \\ \left(1-\alpha_g\right)^{-2.65}\left(1-\alpha_g\right)\mathrm{Re} \le 1000 \\ 0.44 \qquad \left(1-\alpha_g\right)\mathrm{Re} \succ 1000 \end{cases} \quad (11)$$

The drag coefficient exerted by the solid phase on the liquid Phase:

$$C_{D.ls} = \frac{24}{\alpha_g \mathrm{Re}}\left[1+0.15\left(\alpha_g \mathrm{Re}\right)^{0.687}\right]\alpha_g^{-0.265} \quad (12)$$

Fig. 1: Two dimensional computational diagram of the EGSB reactor [7]

Table 2: Operating Conditions applied in this research

Working Condition	Inlet Velocity (m/s)	HRT (h)	Mass fraction of Glucosein feed
C1	0.014	1	0.008
C2	0.0069	2	0.008
C3	0.0034	4	0.008
C4	0.0034	4	0.006
C5	0.0034	4	0.004
C6	0.0034	4	0.002

The lift force acting perpendicular to the direction of the relative motion of the two phases is given by:

$$M_{L,\lg} = C_L p_l \alpha_g (u_g - u_l) \times (\nabla \times u_l) \quad (13)$$

$$M_{L,ls} = C_L \rho_l \alpha_s (u_s - u_l) \times (\nabla \times u_l) \quad (14)$$

Where C_L is the lift coefficient and has a value of 0.5. The interphase momentum transfer between the two dispersed phases, as well as virtual mass force and turbulent dispersion force between the continuous phase and the dispersed phases are all neglected in this study.

Numerical Solution: The finite volume method is used as the numerical technique. The momentum and continuity equations are discretized using finite volumes. For efficient use of computational time, our simulation of the EGSB reactor exploits the symmetric geometry of the reactor and simulates half the geometry in a two-dimensional surface. The simulation results vary little with grid density so truncation errors in the numerical simulation can be neglected. The geometry and the meshes are generated by an in-house code. Therefore, a

two-dimensional computational domain of the complete geometry of the EGSB reactor was devised with 14,440 cells, 29,780 faces and 15,341 nodes and the solution of the model is independent from the number of them (Figure 1). The initial sludge bed was packed with granular solids with a volume fraction of 0.5. The reactor wastewater inlet was modeled with a velocity-inlet boundary condition and the outlet was set as a pressure outlet boundary condition. All other solid surfaces were defined by wall boundary conditions with no slip. The simulation was operated in unsteady state conditions with time step sides equal to 0.001 s. The convergent solution was defined as the solution for which the normalized residual for all variables was less than 1×10^{-3}, except continuity that was less than 1×10^{-4} and the calculated outflow rate had reached a constant value.

To obtain hydrodynamic information from the EGSB reactor, six unsteady state simulations at different up-flow velocity matched to hydraulic retention time (HRT) and mass fraction of glucose were conducted in Table 2.

RESULT AND DISCUSSION

To predict the glucose consumption and biohydrogen production, ethanol-type fermentation reactions were included in the species transport and reaction models via the CFD codes. It is shown that at the beginning of the reaction, mass transfer mainly occurred

In the sludge bed to region because of liquid-solid mixing. (Figure 2) Then with increasing production and release of biogas, the mass transfer was up-warded. This was caused by high turbulence due to intensive mixing. Thus, the efficiency of mass transfer is higher than in other regions, meaning that more glucose will be degraded.

Figure 3 presents the mass fraction of hydrogen production, predicted by the CFD simulation of this research. Hydrogen initial production in the bed region to release may be readily seen from this result. The distribution of gas volume fraction is heterogeneous and mainly distributed about the middle.

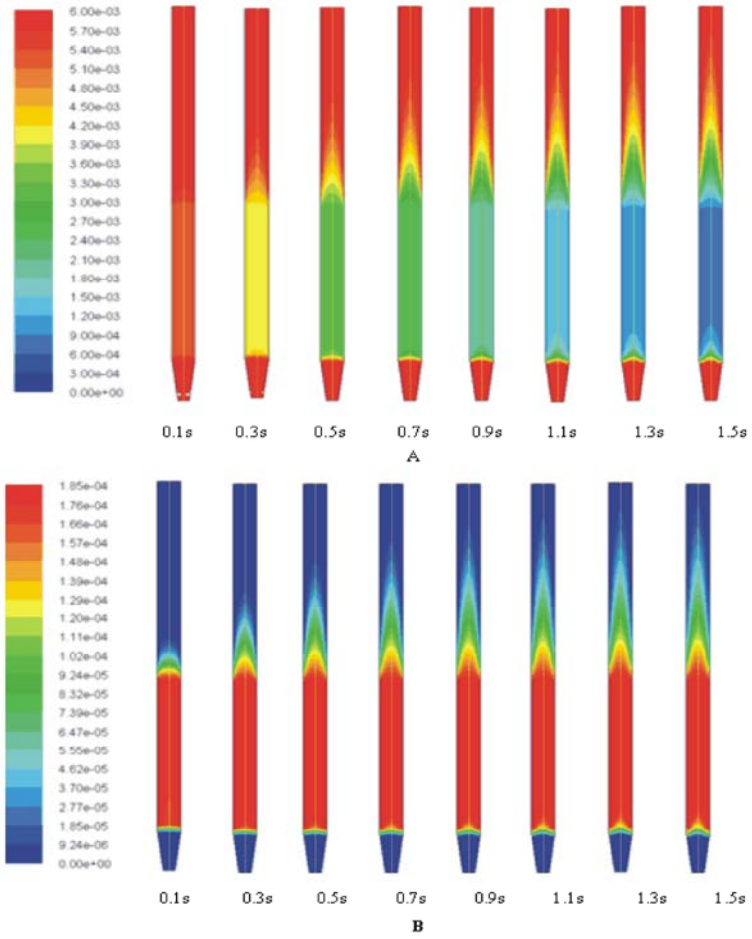

Fig. 2: Contours of species of mass fraction (C4 operating condition) A. glucose; B.ethanol

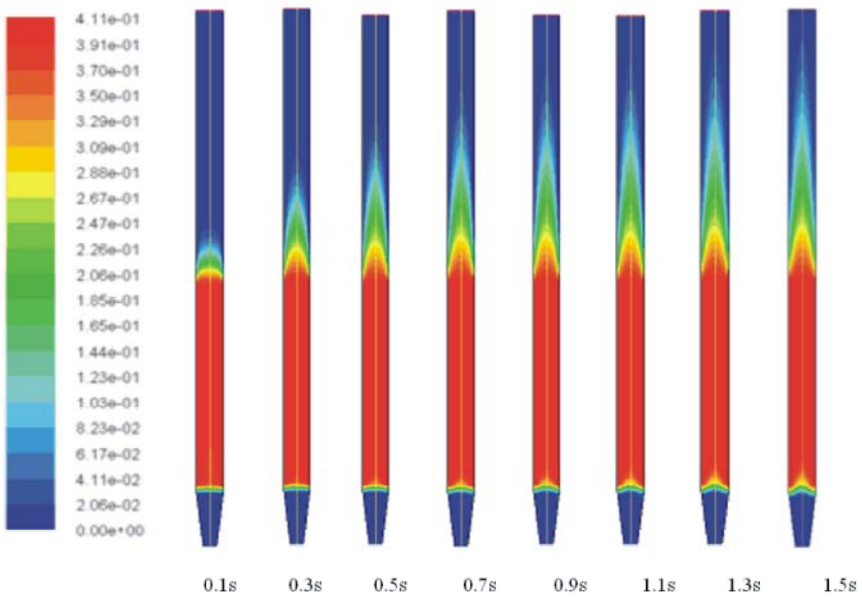

Fig. 3: Contours of mass fraction of hydrogen production in C4 operating condition of Table 2.

This non-homogeneity is caused by the circular liquid flow under the liquid-gas interaction.

The strategy of operation for the hydrogen production experiments utilizing the laboratory-scale H2-producing EGSB reactor was displayed in Table 2. Figures 4A and B show the relationship between the experimental biohydrogen production rate [7] and the outlet hydrogen Mass Flow Rate (MFR) in simulation. From experimental data (see part B of Figure-4) it may be seen that HRT, being related to the water up-flow velocity, affected biohydrogen production. When the HRT exceeded 2h, the hydrodynamic behavior demonstrated was suitable for biohydrogen production. This was due to this behavior which gave an appropriate velocity distribution to maximize inter-phase interactions. By integrating this information with the previous simulation results, a qualitative relationship between hydrodynamics and biohydrogen production might be obtained. In addition, using this reaction model, the response of biohydrogen production with varied inlet mass fraction of glucose in simulation has predictive and directive functions for experimental control and operation (see part A of Figure-4).

CONCLUSION

In this paper, biotreatment of a gas-liquid-solid system has been developed where a CFD code is utilized to investigate its hydrodynamics and reaction kinetics. According to the results of this analysis, the present method is suitable for continuous flow systems. In addition, the results revealed that hydraulic retention time (HRT) have significant effect on hydrogen production. This meant that this factor might be utilized as a key one to control the hydrogen production.

REFERENCES

1. Eduardo, A., B. Aruana, D. Marci and B. Edson, 2009. Anaerobic fluidized bed reactor with expanded clay as support for hydrogen production through dark fermentation of glucose, International Jounal of Hydrogen Energy, 34: 783-790 .
2. Dasd, T., 2001. Hydrogen production by biological process: a survey of literature, .Int J Hydrogen Energy, 26: 13-28.
3. Kapdan, I.K. and F. Kargi, 2006. Bio-hydrogen production from waste materials, Enzyme Microb Technol., 38: 569-82.
4. Puyol, D., A.F. Mohedano, J.L. Sanz and J.J. Rodriguez, 2009. Comparison of UASB and EGSB performance on the anaerobic biodegradation of 2,4-dichlorophenol, Chemosphere, 76: 1192-1198.
5. Maure, F., A. Pio and J. Nicolas, 2009. Heterogeneous anaerobic biofilm reactor models application to UASB , EGSB and AFB reactor, 10th International Symposium on Process Engineering, PSE .

6. Ting-Ting, R., M. Yang, N. Bing-Ji and Y. Hang-Qing, 2009. Hydrodynamics of upflow anaerobic sludge blanket reactors, American Institude of Chemical Engineering, 55: 516-528
7. Xu, W., D. Jie, G. Wan-Qian and R. Nan-Qi, 2010. A hydrodynamics-reaction kinetics coupled model for evaluating bioreactors derived from CFD simulation, Bioresource Technology, 101: 9749-9757 Expected.
8. Guo, W.Q., N.Q. Ren, X.J. Wang, W.S. Xiang, Z.H. Meng, J. Ding, Y.Y. Qu and L.S. Zhang, 2008. Biohydrogen production from ethanol-type fermentation of molasses in an expanded granular sludge bed (EGSB) reactor, Int. J. Hydrogen Energy, 33: 4981-4988.
9. Mu, Y. and Y. Yu Hang-Qing, 2006. Biological hydrogen production in a UASB reactor with granules. I. Physicochemical characteristics of hydrogen-pro-ducing granules, Biotechnol Bioeng, 94: 980-985.